Electronic Supplementary Material (ESI) for Journal of Materials Chemistry A.

Supplementary Information

Composite Anode for Fluoride-Ion Batteries Using Alloy Formation and Phase Separation in Charge and Discharge Processes

Nakayama et al.

Note S1. To clarify the specific redox reactions at the (In + LaF_3) anode during multiple charge-discharge cycles, we performed STEM observations after 10 cycles (discharged state) and 10.5 cycles (charged state). Fig. S1 shows the charge and discharge curves of a thin-film-type battery for 10 cycles, and Fig. S2 shows STEM data obtained after 10 cycles. Although the microstructure is complicated and a certain amount of oxygen is detected (indicating undesired oxidation and/or hydration of La), the presence of In and LaF_3 can be seen, as seen after the first cycle. After 10.5 cycles (discharged state), as shown in Figs. S3 and S4, we can identify In_3La together with nanosized LaF_3, although a small amount of In is also found. These STEM results indicate that the formation of In_3La and phase separation to (In + LaF_3) are repeated during multiple cycles, while the microstructure becomes increasingly complicated, as schematically shown in Fig. S5.

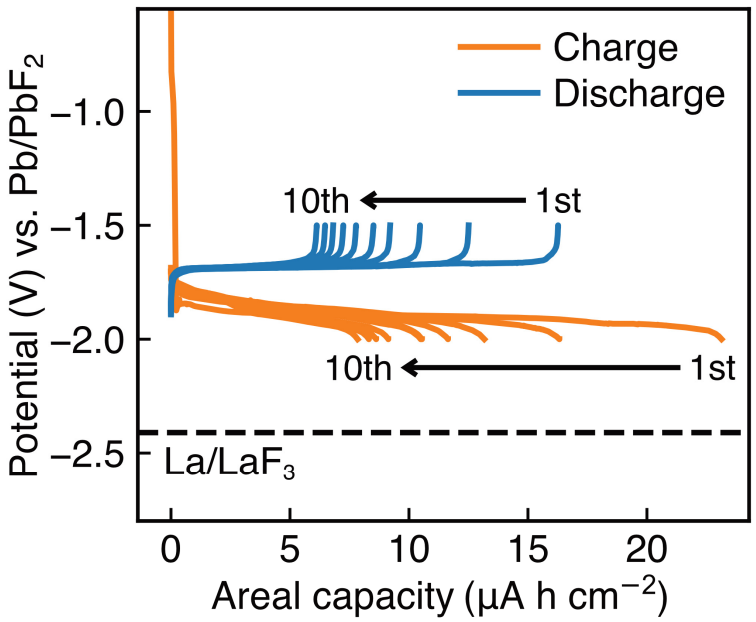

Figure S1. Charge-discharge curves of a thin-film-type fluoride-ion battery for 10 cycles.

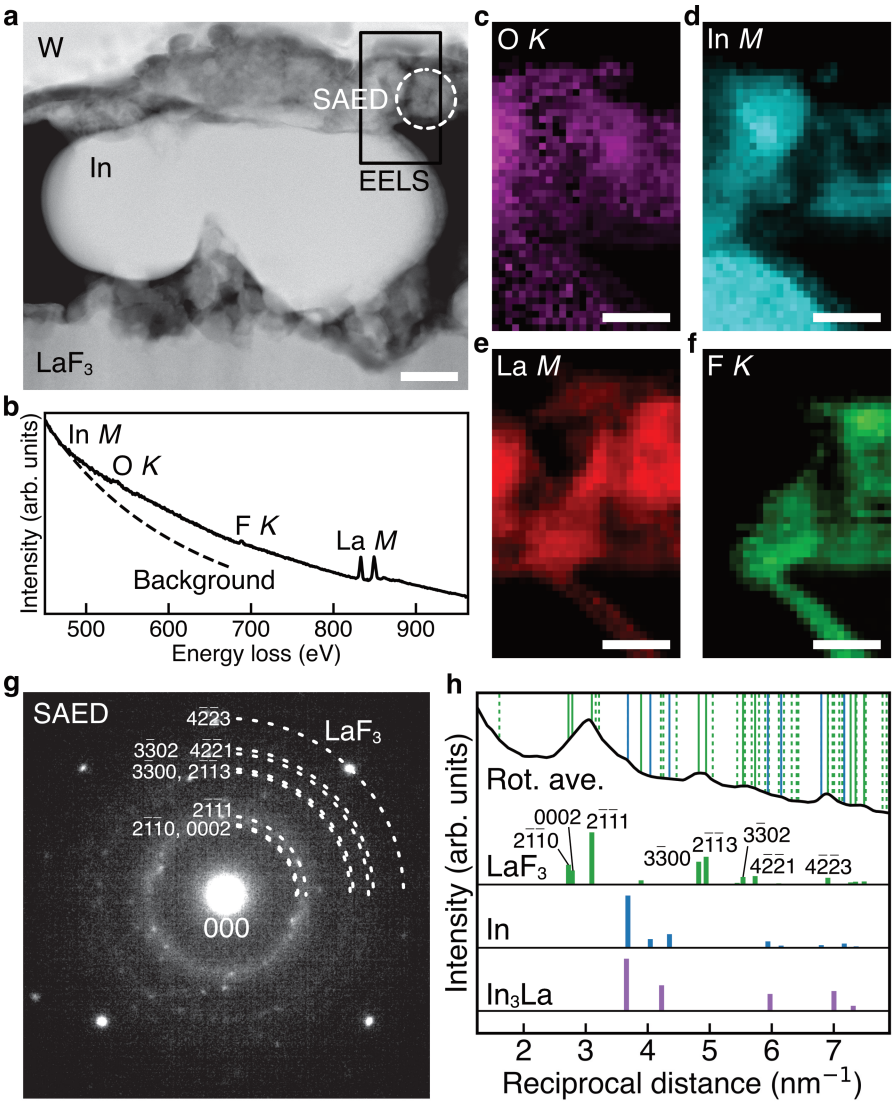

Figure S2. STEM analysis of the (In + LaF_3) anode after 10 cycles (discharged state). (a) ADF STEM image. (b) EELS spectrum obtained from the region surrounded by the rectangle in (a). (c)–(f) O *K*-, In *M*-, La *M*-, and F *K*-edge intensity maps, where the complementary distributions of (d) and (e) indicate a spatial separation of La and In. (g) SAED pattern obtained from the dashed circle region in (a). (h) Rotational average of (g). The scale bar in (a) is 200 nm.

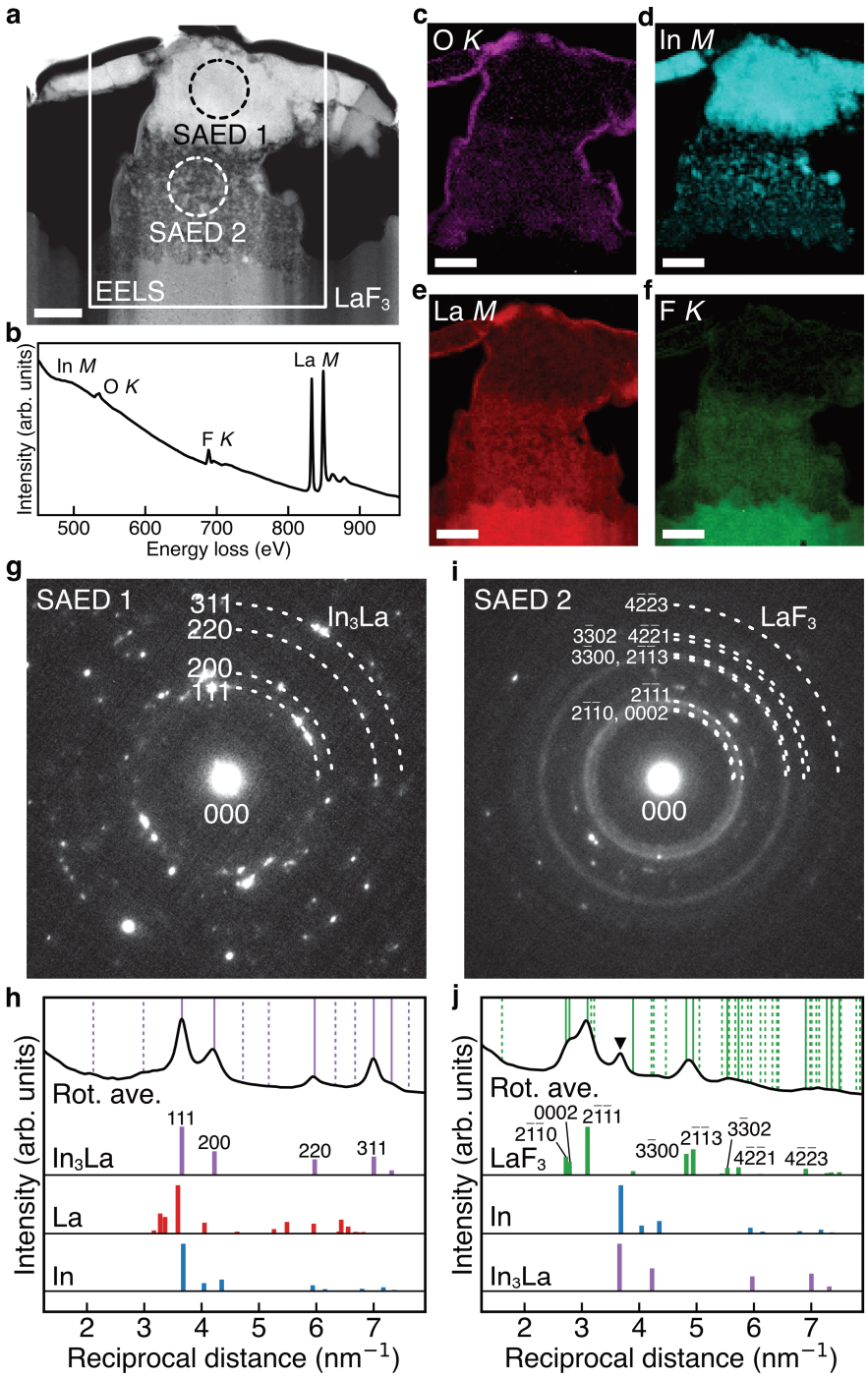

Figure S3. STEM analysis of the (In + LaF_3) anode after 10.5 cycles (charged state). (a) ADF STEM image. (b) EELS spectrum obtained from the rectangle region in (a). (c)–(f) O *K*-, In *M*-, La *M*-, and F *K*-edge intensity maps. (g) SAED pattern obtained from the region enclosed by the black dashed circle in (a). (h) Rotational average of (g). (i) SAED pattern obtained from the region enclosed by the white dashed circle in (a). (j) Rotational average of (i), where the peak indicated by the arrowhead can be assigned to both In and In_3La (see also Fig. S4). The scale bars in (a) and (c)–(f) are 200 nm.

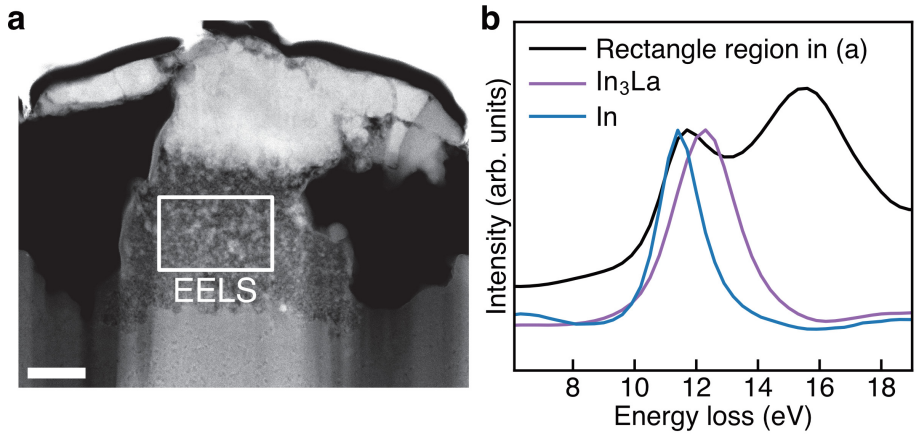

Figure S4. Additional STEM analysis of the (In + LaF_3) anode after 10.5 cycles (charged state). (a) ADF STEM image. (b) EELS spectrum in the low-loss region obtained from the region enclosed by the rectangle in (a), together with referential spectra of In and In_3La. The first peak of the spectrum obtained from the rectangle region is located between the peaks of In and In_3La, which suggests that both In and In_3La are contained in this region. The second peak originates from LaF_3. The scale bar in (a) is 200 nm.

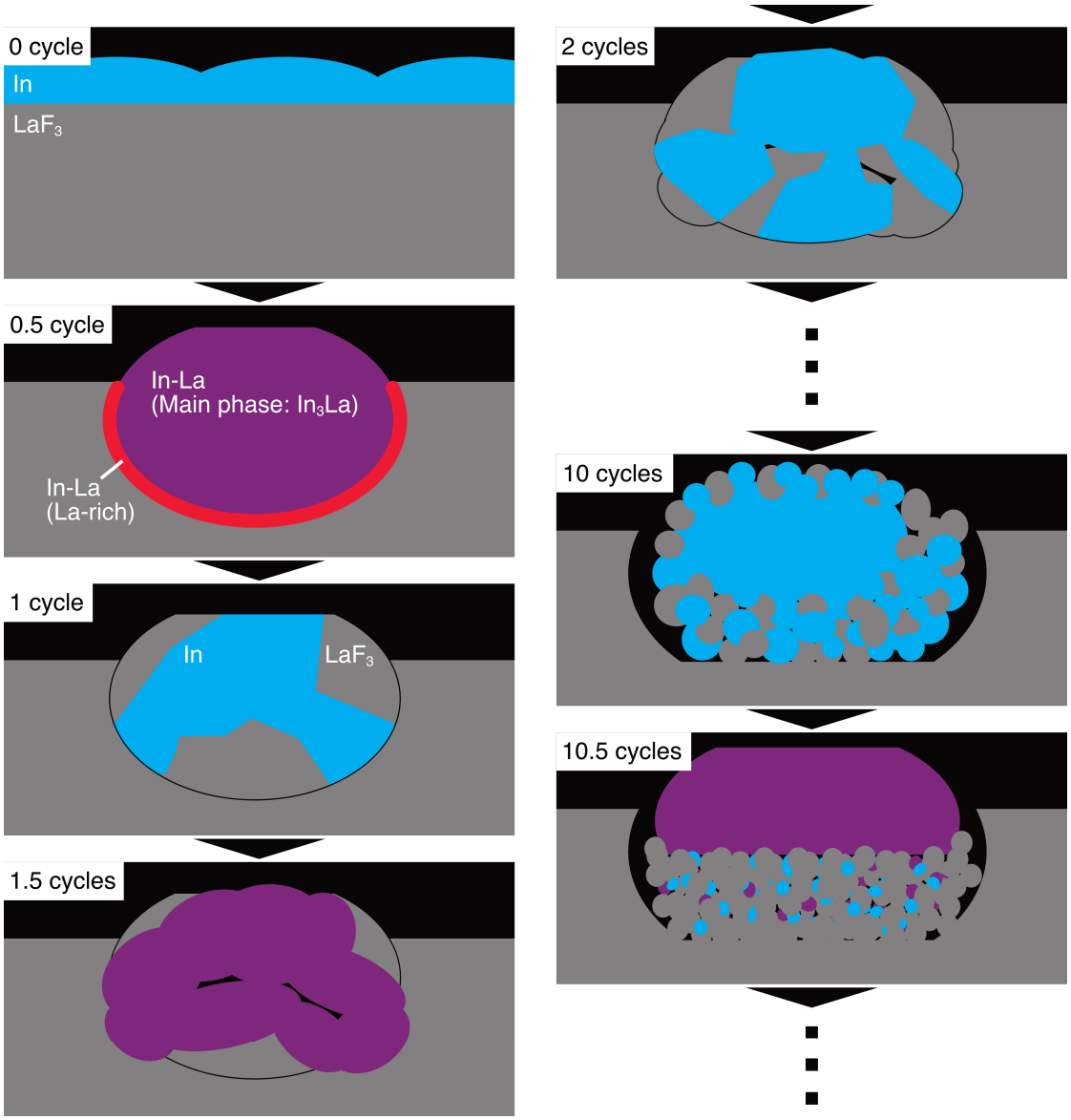

Figure S5. Schematic of the proposed microstructure evolution during charge-discharge cycles. For simplicity, oxidation and hydration of La are omitted.

	Formation energy per atom (eV)	Formation energy per La atom (eV)	Expected potential shift (V)
In_3La	-0.476	-1.904	0.635
In_2La	-0.503	-1.509	0.503
In_5La_3	N/A	N/A	N/A
InLa	-0.505	-1.010	0.337
$InLa_2$	-0.354	-0.531	0.177
$InLa_3$	-0.294	-0.392	0.131

Table S1. Calculated internal energies of formation of In-La intermetallic phases[1] (cf. Materials Project[2]) and expected magnitudes of the potential shift.

References

1. Okamoto, H. In-La (indium-lanthanum). *J. Phase Equilib.* **24**, 93-93 (2003).

2. Jain, A. et al. Commentary: The Materials Project: A materials genome approach to accelerating materials innovation. *APL Mater.* **1**, 011002 (2013).